International Journal of Heat and Mass Transfer 165 (2021) 120616

Contents lists available at ScienceDirect

International Journal of Heat and Mass Transfer

journal homepage: www.elsevier.com/locate/hmt

Computationally-efficient thermal simulations of large Li-ion battery packs using submodeling technique

Vishnu V. Ganesan, Ankur Jain*

Mechanical and Aerospace Engineering Department, University of Texas at Arlington, Arlington, TX, USA

ARTICLE INFO

Article history:
Received 20 July 2020
Revised 23 September 2020
Accepted 17 October 2020

Keywords:
Li-ion cells
Thermal management
Thermal simulations
Sub-modelling technique

ABSTRACT

Accurate and rapid prediction of temperature distribution in a large Li-ion battery pack comprising thousands of cells is critical for ensuring safety and performance of battery packs for electric vehicles. Due to the multiscale geometry and the large number of individual cells in an automotive battery pack, full-scale thermal simulations typically take a long time to complete. Approaches for rapidly computing the temperature field in a large battery pack without significant loss of accuracy is, therefore, a key technological need. This paper presents thermal simulations of a large, air-cooled Li-ion battery pack containing thousands of individual cells using the submodeling technique. A coarse model that neglects fine geometrical details is first solved, and the results are used to solve a more detailed sub-model. It is shown that this approach results in 7X reduction in computation time while preserving the accuracy of the predicted temperature field. Trade-offs between computation time and accuracy are examined. The submodeling technique is used to investigate the thermal design of a large Li-ion battery pack, including the effect of discharge rate and coolant flowrate on temperature field, and the thermal response to a pulsed spike in discharge rate. Limitations of the submodeling technique are discussed. The technique discussed here is a general one, and may help significantly reduce computation time for thermal design and optimization of large, realistic Li-ion battery packs.

1. Introduction

Li-ion cells are used widely for energy storage and conversion in a variety of engineering applications. Compared to other storage technologies, Li-ion cells offer superior energy density, power density and cycling performance [1]. However, Li-ion cells are very temperature sensitive, and thermal management of Li-ion cells and battery packs remains a key technological challenge [2,3]. The poor thermal conductivity of Li-ion cells [4] results in high temperature rise even for moderate heat generation rates. Overheating of cells can lead to initiation of decomposition reactions inside the cell that eventually leads to fire and explosion due to thermal runaway [5]. Li-ion cells are also known to perform poorly at low temperature, which is a key concern for operation in cold climates [6].

Li-ion cells are typically combined in series and/or parallel to form a battery pack. Depending on the power requirement, the number of cells in a pack may range from a few (eg. power tools) to thousands (eg. electric vehicle). In a typical automotive battery pack, a number of individual cells are arranged in series/parallel to form a module [7]. In turn, several modules are assembled together to form the entire battery pack. Several thousands of cells are used in a single automotive battery pack [7]. An appropriately designed thermal management system must be provided to ensure sufficient and uniform cooling of the battery pack. Since experimental measurements in a battery pack may be cumbersome and expensive, computational tools for predicting temperature rise in a battery pack are very important for design optimization. Accurate thermal modeling is also important for run-time battery management during operation. Numerical simulation tools solve the underlying mass, momentum and energy conservation equations through a variety of methods. Through the ability to handle complex geometries, such simulation tools offer an attractive option compared to analytical solutions that can be mathematically complicated [8-9] and limited only to simplified geometries.

A number of papers have presented numerical computation of temperature rise in a Li-ion battery pack. While the computation time is reasonably small for small battery packs, such as those for a hoverboard [10] or a laptop [11], efficient and rapid simulation remains a key challenge for large automotive battery packs comprising thousands of cells where meshing and computation may be time-consuming due to the existence of multiple length-scales. Several papers have presented simulation-based temperature prediction for large battery packs. For example, thermal performance

* Corresponding author.
E-mail address: jaina@uta.edu (A. Jain).

https://doi.org/10.1016/j.ijheatmasstransfer.2020.120616
0017-9310/

Nomenclature

C_p	Heat capacity (J/(kgK))
g	acceleration due to gravity (m/s^2)
k	Thermal conductivity (W/(mK))
p	pressure (N/m^2)
Q	Internal heat generation rate (W/m^3)
t	time (s)
V	Velocity (m/s)
μ	Viscosity (kg/(ms))
ρ	Density (kg/m^3)

of an air-cooled battery pack comprising 24 Li-ion cells was simulated [12]. Using around 6 million nodes, this simulation was reported to take around 53 h to complete. In a similar work [13], thermal-fluid simulations were carried out on a two-dimensional model of a Li-ion battery pack. This simulation was reported to take around 9 h. Numerical simulations have been presented for a water-cooled battery pack containing 14 cells [14]. In another paper, simulation of a 5000 cell battery pack was carried out using a two-step projection method, where mass continuity and Navier Stokes equations for the coolant liquid were solved first, followed by computation of energy conservation equations [15]. Unfortunately, the computation time was not specified, but was probably very large. A lumped capacitance simulation model for the battery pack has also been presented [13,16]. While this approach offers rapid computation of temperature, it suffers from the approximations associated with lumped modeling. In some papers, thermal simulation was carried out only for a small portion of the pack instead of the entire pack [17-18]. While this approach computed temperature within a reasonable time, the results may not be representative of the entire battery pack. Specifically, non-uniformity with a battery pack is important to understand, and cells not being adequately cooled must be identified, which can only be done through a simulation of the entire battery pack.

The literature cited above clearly highlights the importance of optimizing thermal simulations for a complex, large-sized Li-ion battery pack. Rapid temperature prediction with acceptable accuracy is a critical need. Trade-offs between computational time and accuracy need to be carefully understood and optimized. Techniques such as submodeling [19], iterative sub-structure method [20] and Model Order Reduction method [21] have been developed for addressing such problems in other applications, but have not been investigated for thermal simulations of Li-ion battery packs.

In the submodeling technique, a global model of the entire geometry of interest is first solved while using a coarse grid and omitting fine geometrical details. A refined local model of the region of interest, also known as a sub-model, is then set up and solved using boundary conditions obtained from the results of the global model [19]. Submodeling is particularly attractive where geometrical features exist over multiple length scales, as is the case in a Li-ion battery pack. The global model can be solved without accounting for finer features, which can later be included in the sub-model, resulting in faster computation with minimal loss of accuracy compared to a full-scale simulation model. The use of submodeling technique has been reported for a number of engineering applications such as metal additive manufacturing [22], microelectronic devices and systems [19,23], aerospace [24] and structural engineering [25]. However, there is a lack of past work on the use of submodeling for thermal simulations of Li-ion battery packs. The considerable geometrical complexity and existence of multiple length scales in a battery pack make submodeling a particularly suitable technique for thermal simulations of Li-ion battery packs.

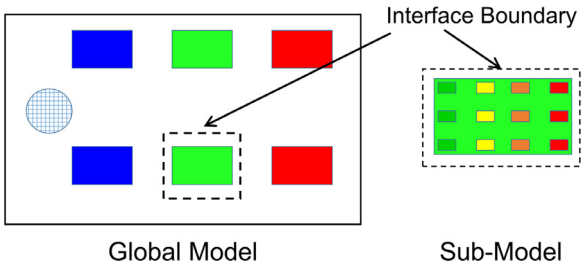

Fig. 1. Schematic of a general sub-modeling thermal/mechanical simulation technique.

This paper presents computationally efficient thermal simulation of a large Li-ion battery pack comprising more than 6800 cells using submodeling technique. It is shown that the computation time can be reduced by around seven times, while incurring minimal error compared to a full-scale model. The submodeling technique is introduced in Section 2.1. The application of this technique for thermal simulation of a representative automotive Li-ion battery pack is discussed in Section 2.2. Results are discussed in Section 3.

2. Sub-modeling

This section introduces the basic concept behind the submodeling technique, and then discusses implementation of submodeling for thermal simulations in a large battery pack.

2.1. Sub-modeling procedure

The fundamental principle behind submodeling is the St. Venant principle [26] which, in the context of mechanical loads, states that two different but statically equivalent loads have nearly the same effect sufficiently far from the load. As a result, one can first solve the displacement field for a coarse model that ignores fine geometrical details, and then transfer the displacement results as boundary conditions to a more detailed submodel of a smaller subset of the region. While developed originally for mechanical stress simulations, the same principle also applies for thermal simulations.

Fig. 1 shows a schematic of a general body, for which computation of thermal/mechanical response to imposed loads is of interest. There may be several multiscale geometrical features within the body, due to which, an outright simulation of the entire body is computationally challenging. Instead of modeling complete details of the geometry within the body and carrying out a numerical simulation of the entire body, the sub-modeling technique first simulates a coarse model that neglects the finer features in the geometry. Results from this simulation are then transferred to a refined region – usually the area where stress concentration or a thermal hotspot may be expected – through the displacement/temperature predicted by the coarse model along the interface boundary. The refined region is referred to as the submodel. Simulation of the sub-model then provides detailed temperature/stress distribution within the submodel. In general, the accuracy of the results depend on how well the coarse model is meshed, since, the greater the number of nodes in the global model, the more accurate will be the information along the interface boundary that is transferred to the submodel. A key advantage of the submodeling technique is that one can focus specifically on certain regions of the geometry, such as those that are expected to produce the highest temperature rise, without the need to simulate fine geometrical details of the entire geometry.

Although submodeling was originally developed for mechanical stress analysis, it is equally effective for thermal and fluid simu-

lations as well. In such a case, results from the global model are transferred to the submodel in the form of fluid velocity and temperature fields on the interface boundary, as shown in Fig. 1.

2.2. Sub-modeling for a Li-ion battery pack

Two specific thermal simulations related to air cooling of Li-ion battery packs are set up using the submodeling technique. The first is a proof-of-concept simulation comprising a relatively small number of Li-ion cells in the battery pack. Once the first simulation is validated, the second simulation addresses a much more complicated and realistic battery pack comprising more than 6800 cells. The implementation of these simulations is described next.

2.2.1. Proof of concept

The general sub-modeling process outlined in Section 2.1 is used for carrying out thermal simulation of a Li-ion battery pack. Sub-modeling is implemented in ANSYS ICEPAK, which uses FLUENT solver for thermal and fluid flow analysis. The simulation solves the following equations representing conservation of mass, momentum and energy, respectively:

$$\nabla.V = 0 \tag{1}$$

$$\rho\left(\frac{\partial V}{\partial t} + (V.\nabla)V\right) = -\nabla p + \mu\nabla^2 V \tag{2}$$

$$\rho c_p\left(\frac{\partial T}{\partial t} + (V.\nabla)T\right) = k\nabla^2 T + Q \tag{3}$$

The proof-of-concept simulation is carried out on a battery pack comprising four modules of ten prismatic Li-ion cells each, for a total of 40 cells. Each cell is sized 80 mm by 80 mm by 3 mm. Each cell is assumed to generate 0.2 W heat, corresponding to a C-rate of 1C [27]. Note that C-rate of a battery is defined as the ratio of the current and the theoretical current that would cause the battery to deliver its rated capacity in one hour [1]. As an example, starting from a fully charged state, batteries discharging at 1C and 2C will completely discharge in one hour and 0.5 hour, respectively. Thermal conduction in a Li-ion cell is known to be orthotropic [4] due to thermal contact resistance between layers in the out-of-plane direction [28]. Therefore, in these simulations, in-plane and out-of-plane thermal conductivity values of 30 W/(mK) and 0.2 W/(mK), respectively, are taken, based on past measurements [4]. The specific heat capacity is assumed to be 860 J/(kgK) [29]. The cells are being cooled by natural convection to the surrounding air, with the gravity vector pointing downwards. The outer surfaces of the battery pack are convectively cooled with a heat transfer coefficient of 100 W/(m^{2}K). The initial temperature of the entire geometry in this, and all subsequent analysis in this paper is assumed to be 20 °C. Implementation of the sub-modelling technique for this simple system is shown schematically in Fig. 2, which shows the full-scale model as well as the global and sub-models for the submodeling technique. In the submodeling technique, a global model is first solved, in which, the four modules are modeled as homogeneous blocks without the details of the ten cells contained in each module. These four blocks have the same thermal properties as the individual cells in the full-scale model. Further, the same external boundary conditions as the fullscale model are applied. Temperature and velocity fields predicted by the global model along the boundaries of the module are then transferred as the boundary conditions for the submodel. Complete details of the cells within each module are included in the sub-model. Results of the submodel provide the complete temperature distribution for each cell in the pack. For validation, a full-scale simulation that directly accounts for each cell in each module in a single simulation is also carried out.

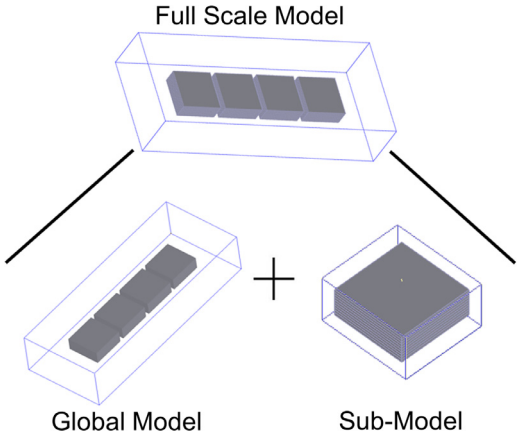

Fig. 2. Schematic showing the implementation of the sub-modeling technique for a proof-of-concept simulation of a small battery pack comprising only 40 prismatic cells.

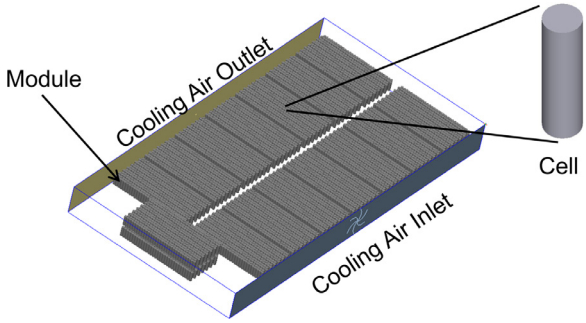

Fig. 3. Picture of a representative air-cooled automotive Li-ion battery pack comprising 16 modules of 427 cells each, for a total of 6832 cells.

2.2.2. Analysis of a realistic automotive battery pack

Submodeling technique is then used for thermal simulation of a much larger, air cooled battery pack that is representative of an electric vehicle battery pack. As shown in Fig. 3, this battery pack comprises 16 modules, each of which contain 427 cylindrical Li-ion cells of 18,650 configuration (18 mm diameter, 65 mm height) arranged in 14 rows. The total number of cells in the pack is 6832. Note that there are two modules located on the left end of the pack in Fig. 3, which are at a different height compared to the other 14 modules. Consistent with experimental measurements [4], thermal conductivity of the cell is assumed to be orthotropic, with axial and radial values of 30 W/(mK) and 0.2 W/(mK), respectively. The pack is cooled by forced convection due to air flow from a fan, as shown in Fig. 3. Air flow rate is specified at the inlet as a boundary condition. The outer boundaries of the battery pack are assumed to be cooled by natural convection. Radiation and natural convection are neglected. A convergence limit of 10^{-10} is used for the energy residual in the simulations.

Two distinct sub-modeling approaches – single-stage and two-stage – shown in Figs. 4(a) and 4(b) are investigated for submodeling of this large battery pack. In both approaches, the global model treats each battery module as a homogeneous solid block with a heat generation rate equivalent to that of all the cells in the module. Simulation of the global model captures the fluid flow around each module, which, in addition to temperature, is then transferred as boundary condition to the region of interest. The single-stage and two-stage approaches differ from each other in how the sub-model is treated. In the single-stage approach, all the cells in the module are included in the sub-model, as shown in Fig. 4(a). On the other hand, in the two-stage approach, as shown in Fig. 4(b), the sub-model comprises a section of the module, which, in turn,

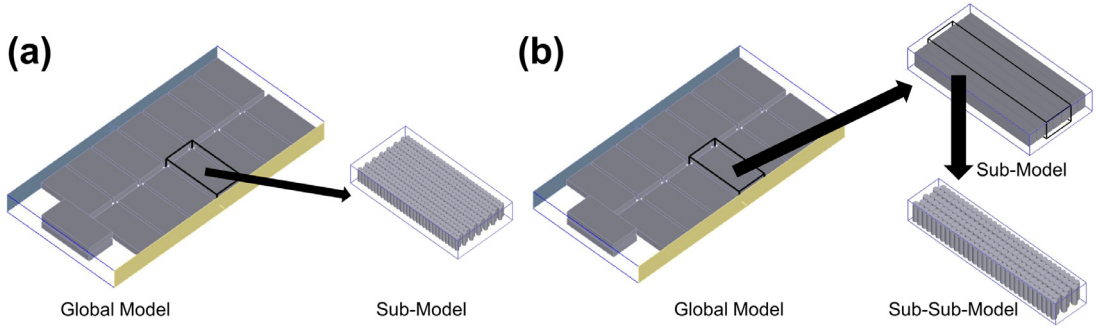

Fig. 4. Schematics showing (a) single-stage and (b) two-stage submodeling of large Li-ion battery pack.

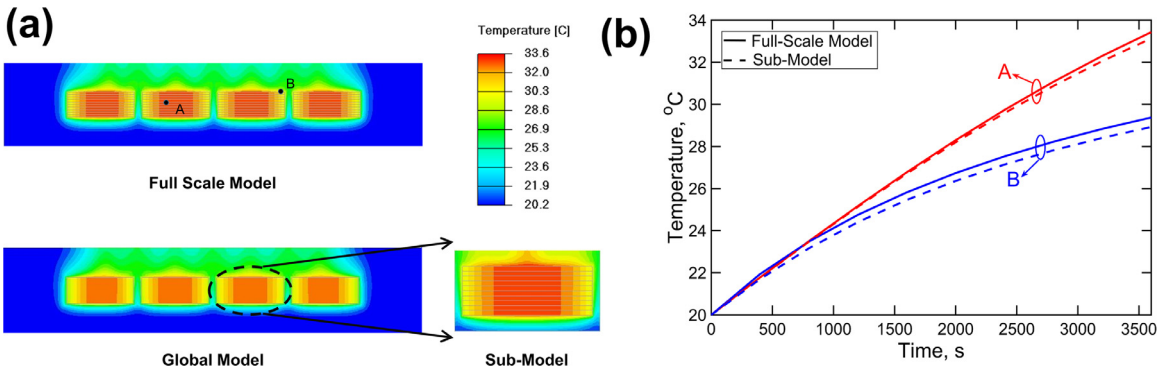

Fig. 5. Results for proof-of-concept simulation: (a) Comparison of computed colorplots for a full-scale modeling and sub-modeling at $t = 3600$ s; (b) Comparison of temperature as a function of time predicted by full-scale modeling and sub-modeling for two different locations A and B in the battery pack. (For interpretation of the references to colour in this figure legend, the reader is referred to the web version of this article.)

leads to a second-stage sub-model that includes the geometrical details of individual cells. The two submodeling approaches are compared with each other, and with a full-scale model in terms of accuracy and computational time.

3. Results and discussion

3.1. Proof-of-concept simulation

Fig. 5 presents a comparison of full-scale modeling with the submodeling technique for the proof-of-concept battery pack with only 40 cells. The C-rate for this case is 1C, with natural convection cooling from cells to surrounding air and forced convective cooling with heat transfer coefficient of 100 W/(m^{2}K) from the outer surfaces of the battery pack. Temperature colorplots at $t = 3600$ s for the two approaches are shown in Fig. 5(a). Both global model and sub-model results are shown for the submodeling technique. Fig. 5(b) presents this comparison in terms of temperature as a function of time at two locations A and B in two different modules in the battery pack. Colorplots in Fig. 5(a) show excellent agreement between the full-scale and sub-modeling techniques. As shown in Fig. 5(b), location A experiences a higher temperature rise due to its location being in the middle of one of the internal modules, whereas temperature at location B is lower due to its more favorable location. In both cases, Fig. 5(b) shows that the submodel is in good agreement with fullscale simulation. The computation time for the submodeling technique is 3.5 h compared to 5 h for the fullscale model. Thus, while taking about 30% lesser computational time, the submodeling technique is able to predict temperature rise with negligible error compared to the full-scale simulation. This is a relatively simple, proof-of-concept simulation that does not fully utilize the capability of the submodeling technique for computational efficiency. Simulation of a more complicated and realistic battery pack is discussed next.

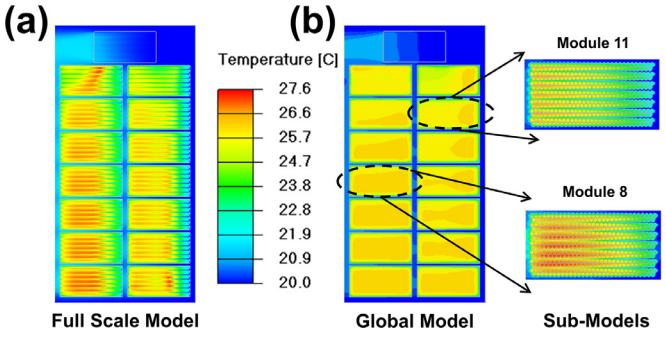

Fig. 6. Results for the large battery pack containing 6832 Li-ion cells: (a) Temperature colorplot for the full-scale model; (b) Temperature colorplots for the submodeling technique, showing colorplots for the global model as well as the submodel. In each case, temperature is plotted at $t = 3000$ s for 1 C discharge rate while the pack is being cooled with 5 m/s air flow.

3.2. Simulation of a large scale battery pack

The submodeling technique is investigated for a much larger and more realistic 6832-cell battery pack described in Section 2.2. Due to the large range of lengthscales in the battery pack geometry, a full-scale simulation is found to require around 10 Million nodes in order to reasonably resolve each of the 6832 cells and obtain mesh independence. This is expected to be very computationally intensive and infeasible for practical applications. As an alternative, submodeling is explored for solving this problem. The battery pack is assumed to operate at 1C discharge rate, corresponding to 0.2 W heat generation in each cell [27]. Note that the volumetric heat generation rate is taken from past measurements on a 2.6 Ahr $LiFePO_4$ cell. The coolant air flowrate is taken to be 5 m/s. Fig. 6 compares results from the submodeling technique with a

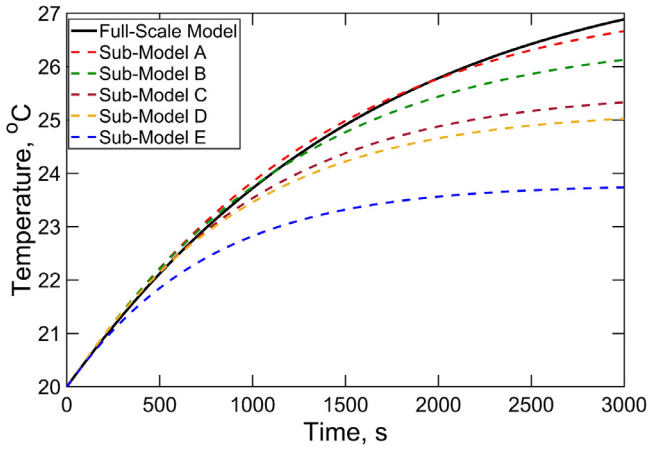

Fig. 7. Temperature at the center of the 8th module in the battery pack as a function of time for the full scale model and five different submodels with varying number of elements. The pack geometry, heat generation rate and cooling conditions are the same as those in Fig. 6.

full-scale simulation for these parameters. Note that in these Figures, the coolant air enters from the right and exits from the left of the battery pack. Fig. 6(a) plots temperature colormap for the entire battery pack at $t = 3000$ s based on a full-scale model. In comparison, sub-modeling results for both global model and submodels for two specific modules are shown in Fig. 6(b) at $t = 3000$ s. The computational time for the submodel is only 20% of the time taken for the fullscale model. Yet, these colorplots show that the sub-modeling technique is able to capture key features of the temperature distribution, including locations of the highest and lowest temperature, as well as finer details of temperature distribution amongst the cells within each module in the submodels.

For a more quantitative comparison between the two techniques, temperature as a function of time for a cell located at the center of the 8th module is plotted in Fig. 7. The discharge rate is 1C and the pack is being cooled with air flow at 5 m/s. Fig. 7 presents results from the fullscale model as well as five different submodeling approaches – A through E – that differ in mesh size. Submodel A has the finest mesh, little over 3 million elements, while Submodel E has the coarsest mesh, less than 16,000 elements. Fig. 7 shows that as the mesh quality in the submodeling approach improves, the results get closer and closer to those predicted by a fullscale simulation. In general, the finer the mesh in the global model of the submodeling technique, the more accurate the result are, although this comes at the price of increased computational time. The fullscale simulation model takes around 150 h to compute due to its very extensive mesh. For Submodel A, with the finest mesh, the computation time is 20% that of the fullscale simulation, with worst-case error of 3% compared to the fullscale simulation. On the other hand, using the coarsest mesh, Submodel E results in a much lower computational time – only 4.5% of the time for fullscale simulation – but also results in greater error – around 46% compared to the fullscale simulation.

This important trade-off between accuracy and computation is investigated further in Fig. 8, which plots the percent error in submodeling compared to fullscale model as well as computation time as a percentage of the time taken by the fullscale model, both as functions of the number of mesh elements in the submodel. Fig. 8 shows that as the mesh gets finer, the results become more and more accurate, but at the cost of increased computation time. As the number of elements increases, the percentage error drops rapidly at first, but then slows down somewhat. On the other hand, the computational time continues to increase almost linearly with increasing number of elements. Depending on the error tolerance

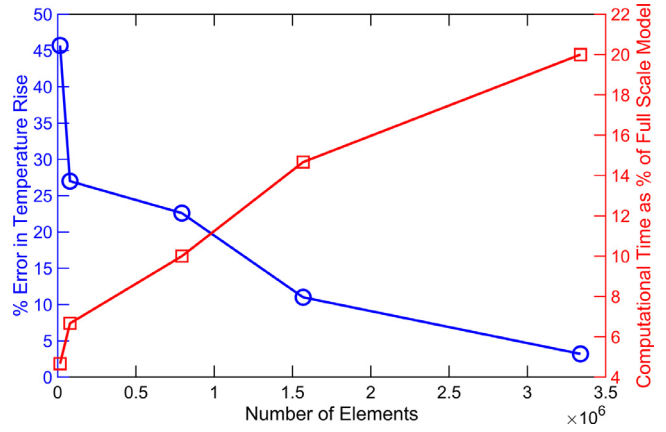

Fig. 8. Error percentage and computation time relative to full scale model for a number of submodels with different number of elements.

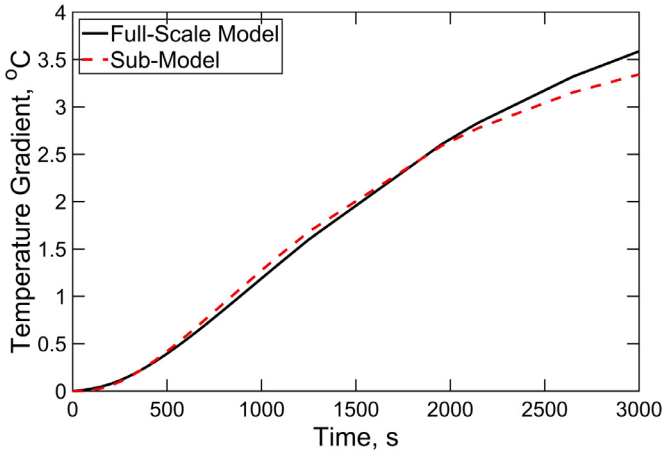

Fig. 9. Temperature gradient within module 8 as a function of time. Results from submodeling technique are compared with the full scale model.

and need for rapid computation in a given application, the submodeling approach could be used with an appropriate balance between error and computation time, as shown in Fig. 8. A reasonable trade-off between the two may exist in the middle of the plot shown in Fig. 8 because increasing the number of elements further does not improve the error very much, while still incurring significant increase in computational time.

Significant temperature non-uniformity is known to exist in Li-ion cells [30], which is generally not desirable as it may lead to electrochemical imbalance and reliability concerns. A comparison of the submodeling technique with fullscale simulations is carried out by plotting the temperature gradient (difference between maximum and minimum temperature) within a module as a function of time. Fig. 9 plots the temperature gradient for module 8 as function of time predicted by the full scale model as well as the submodel. Geometry and other conditions are the same as Fig. 6. The curves in Fig. 9 are close to each other, indicating the capability of the submodeling technique to accurately capture the temperature gradient within the module.

3.3. Single-stage vs two-stage submodeling

All the simulations described so far use a single-stage submodel to fully resolve the simulation geometry. It is also possible to use multi-stage submodeling to reduce the overall computation time, although there may be greater loss of accuracy. Multistage submodeling may be particularly helpful for very compli-

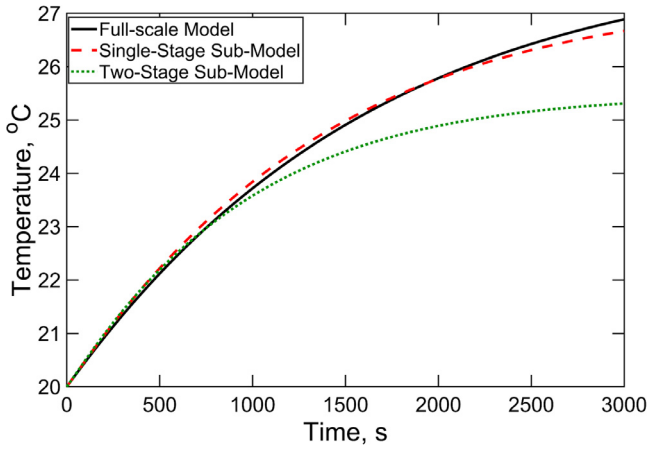

Fig. 10. Comparison of temperature at center of 8th module as a function of time computed by single-stage and two-stage submodeling simulations with fullscale simulation.

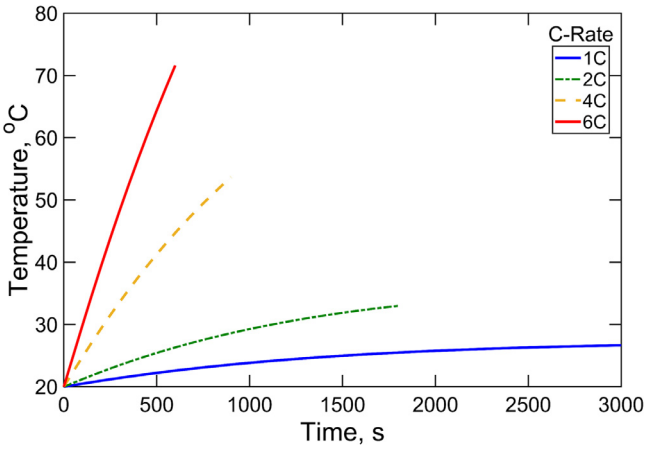

Fig. 11. Temperature at the center of module 8 in the battery pack as a function of time for four different discharge rates, with 5 m/s coolant air flow in each case.

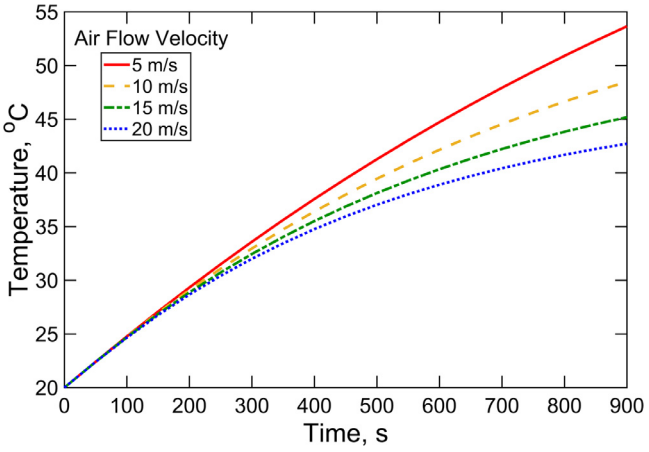

Fig. 12. Temperature at the center of module 8 in the battery pack as a function of time for four different coolant air velocities, with constant 4C discharge rate in each case.

cated geometries that can not be fully resolved with just one submodel. In two-stage submodeling, as shown schematically in Fig. 4, results from the global are used to solve a first-stage submodel, which is then used to solve an even smaller, second-stage submodel. This approach is investigated and compared against fullscale and single-stage submodeling for 1C discharge of the 6832-cell battery pack cooled with 5 m/s air flow rate. Results are shown in Fig. 10 in terms of temperature at the center of module 8 as a function of time. Fig. 10 shows that while the single-stage submodeling approach agrees nearly exactly with the full scale model, there is around 25% error in the two-stage submodel. This is accompanied by a 10% improvement in computation time compared to the single-stage submodeling approach. In order to determine whether two-stage submodeling is attractive, the reduction in accuracy must be weighed against the improvement in computation time when using two-stage submodeling compared to single-stage submodeling. In the present context, given the significant reduction in computation time even for single-stage submodeling, the additional effort for setting up two-stage submodeling may not be justified, unless reducing the computation time to the minimum possible is extremely important.

3.4. Investigation of effect of discharge rate and coolant flowrate

The submodeling technique is used for thermal evaluation of different thermal design scenarios in a Li-ion battery pack. Specifically, the impact of discharge rate and coolant air flow on temperature distribution in the battery pack is evaluated.

Heat generation rate in a Li-ion cell is a strong, quadratic function of the discharge rate – the larger the rate at which energy is drawn from the cell, the larger is the heat generation rate [27]. As a result, the C-rate of the battery pack is a critical performance parameter that must be chosen to balance the objectives of meeting the external load on the battery and keeping the battery temperature within safe limits. The submodeling technique is used to compute temperature distribution in the 6832-cell battery pack operating at four different discharge rates. In each case, coolant air flow at 5 m/s speed is considered and the entire discharge process from fully charged to fully discharged is simulated. Fig. 11 plots the temperature at center of module 8 in the battery pack as a function of time for these cases. Note that the larger the discharge rate, the shorter is the time period for the battery to fully discharge. As expected, the submodeling technique shows a non-linear increase in temperature with increasing C-rate. The peak temperature rise at 1C discharge is reasonably small, and rises significantly with increasing C-rate despite the shorter discharge time. At 6C discharge, the battery temperature may exceed the safety limits to prevent thermal runaway. Results shown in Fig. 11 indicate that the C-rate in the battery pack must be limited, or, alternately, the coolant flowrate must be increased to keep the battery pack temperature within a safe limit.

Fig. 12 investigates the impact of varying the coolant air velocity at a constant C-rate of 4C. The geometry and other properties are the same as previous Figures for the 6832-cell battery pack. A plot of temperature as a function of time at the center of the 8th module in the battery pack presented in Fig. 12 shows that the temperature field approaches steady state faster with larger air flow rate, which is consistent with the expectation of greater rate of heat removal from the pack at larger air flow rates. In addition, as expected, temperature curve reduces as the air flow rate increases, due to improved heat removal.

Plots such as Figs. 11 and 12 provide helpful design guidelines for thermal management and operation of the battery pack. These data can be used to carefully balance performance (battery load and C-rate) with safety (temperature rise). These results are obtained with significantly reduced computational burden compared to fullscale simulations. The reduction in computational time may enable capabilities in design, operation and thermal management of the battery pack that are simply not possible when relying only on time-consuming fullscale simulations.

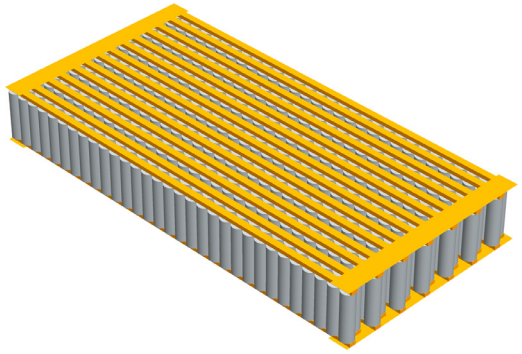

Fig. 13. Schematic of a single module showing the Copper connectors for electrical interconnection of cells.

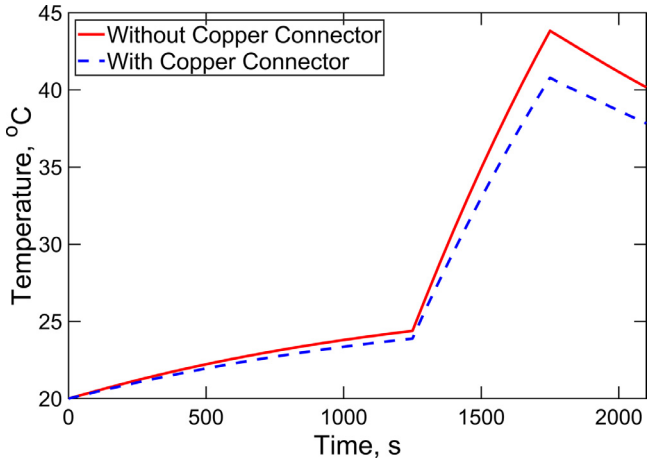

Fig. 14. Impact of the presence of Copper connectors on temperature at center of 8th module during an intermittent spike in discharge rate, which changes from 1 C to 4 C between t = 1250s and t = 1750s.

Finally, the impact of metal interconnection present in battery modules on temperature rise during a spike in heat generation rate is investigated. Cells in each module are typically connected in a series-parallel combination using metal connectors. Fig. 13 shows a representative schematic of the metal connectors used to electrically connect cells to each other. The connectors are typically made of a metal such as Copper that has high electrical and thermal conductivity. A past paper has demonstrated the importance of the metal connector on temperature distribution in the cells [31]. However, this study was carried out on a pack of only five cells. The impact of metal connectors in a large 6832-cell battery pack such as the one analyzed in previous Figures is investigated here. For this purpose, temperature distribution in the pack is compared with and without the presence of Copper connectors of 5 mm thickness and 9 mm width. A spike in discharge rate is modeled, wherein the battery pack discharges at 1 C for the discharge duration, except between t = 1250s and t = 1750s, during which, the discharge rate spikes to 4 C. In such a case, it is expected that the thermal capacitive effect of the Copper connectors may help limit temperature rise during the spike. Fig. 14 presents a comparison of temperature rise at center of the 8th module in the battery pack with and without the Copper connectors for the discharge process described above using the submodeling technique. Fig. 14 shows a lower temperature rise due to the presence of the Copper connectors, which is attributable to the ability of the connectors to absorb the extra heat generated during the C-rate spike. This is consistent with a past study on a five-cell pack [31] but has been demonstrated in the present work for a much larger and more realistic battery pack. Fig. 14 demonstrates the capability of the submodeling technique to compute temperature fields in the battery pack for various design scenarios much faster than fullscale modeling.

In summary, the large number of cells and other geometrical complexities in a realistic Li-ion battery pack present considerable challenges in thermal simulations. A full scale thermal simulation is often computationally infeasible. The submodeling technique discussed in this paper overcomes some of these challenges and offers a means to balance computation time and accuracy. Depending on the computational resources available and accuracy requirements, the submodeling technique may be adapted to fit specific needs of the problem at hand. It must be noted that the submodeling technique may not be effective in the presence of nonlinear phenomena such as temperature-dependent thermal properties. Further, inaccurate transfer of boundary conditions from the global model to the submodel may also result in inaccurate results. This may happen, for example, for very complicated geometries.

4. Conclusions

While submodeling has been used extensively in other engineering applications, particularly for mechanical stress simulations, its use for thermal simulations of Li-ion battery pack has not been described in the past. The present work addresses this aspect, and shows that submodeling-based thermal simulations of large battery packs may dramatically reduce computational time (7X in the present case) while preserving accuracy. The submodeling technique is demonstrated on a large 6832-cell battery pack. The work described in this paper may help speed up thermal design and optimization, as well as run-time thermal control of large, realistic Li-ion battery packs, such as those used in electric vehicles.

Credit authorship contribution statement

Vishnu Ganesan – Methodology, Formal Analysis, Investigation, Data Curation, Visualization

Ankur Jain – Conceptualization, Methodology, Supervision, Project Administration, Data Curation, Visualization, Funding Acquisition, All authors contributed towards writing original draft and review/editing.

Declaration of Competing Interest

Both authors hereby declare that they do not have any conflict of interest as described by Elsevier's policies (http://www.elsevier.com/conflictsofinterest).

Acknowledgments

This material is based upon work supported by CAREER Award No. CBET-1554183 from the National Science Foundation.

References

[1] K.W. Beard, Handbook of Batteries, 5th Ed, McGraw-Hill, 2019.
[2] T.M. Bandhauer, S. Garimella, T.F. Fuller, A critical review of thermal issues in Li-ion batteries, J. Electrochem. Soc. 158 (2011) R1–R25.
[3] K. Shah, V. Vishwakarma, A. Jain, Measurement of multiscale thermal transport phenomena in Li-ion cells: a review, J. Electrochem. Energy Convers. Storage 13 (2016) 1–13 030801.
[4] S.J. Drake, D.A. Wetz, J.K. Ostanek, S.P. Miller, J.M. Heinzel, A. Jain, Measurement of anisotropic thermophysical properties of cylindrical Li-ion cells, J. Power Sources 252 (2014) 298–304.
[5] I. Esho, K. Shah, A. Jain, Measurements and modeling to determine the critical temperature for preventing thermal runaway in Li-ion cells, Appl. Therm. Eng. 145 (2018) 287–294.
[6] S.S. Zhang, K. Xu, T.R. Jow, The low temperature performance of Li-ion batteries, J. Power Sources 115 (2003) 137–140.
[7] G. Xia, L. Cao, G. Bi, A review on battery thermal management in electric vehicle application, J. Power Sources 367 (2017) 90–105.

[8] K. Shah, S.J. Drake, D.A. Wetz, J.K. Ostanek, S.P. Miller, J.M. Heinzel, A. Jain, An experimentally validated transient thermal model for cylindrical Li-ion cells, J. Power Sources 271 (2014) 262–268.
[9] D. Chalise, K. Shah, R. Prasher, A. Jain, Conjugate heat transfer analysis of thermal management of a Li-ion battery pack, J. Electrochem. Energy Convers. Storage 15 (2018) 1–8 011008.
[10] A. Prasad, M. Parhizi, A. Jain, Experimental and numerical investigation of heat transfer in Li-ion battery pack of a hoverboard, Int. J. Energy Res. 43 (2019) 1802–1814.
[11] A. Mills, S. Al-Hallaj, Simulation of passive thermal management system for lithium-ion battery packs, J. Power Sources 141 (2005) 307–315.
[12] L.H. Saw, Y. Ye, A.A.O. Tay, W.T. Chong, S.H. Kuan, M.C. Yew, Computational fluid dynamic and thermal analysis of Lithium-ion battery pack with air cooling, Appl. Energy 177 (2016) 783–792.
[13] R. Mahamud, C. Park, Reciprocating air flow for Li-ion battery thermal management to improve temperature uniformity, J. Power Sources 196 (2011) 5685–5696.
[14] M.S. Patil, J.-.H. Seo, S. Panchal, S.-.W. Jee, M.-.Y. Lee, Investigation on thermal performance of water-cooled Li-ion pouch cell and pack at high discharge rate with U-turn type microchannel cold plate, Int. J. Heat Mass Transfer 155 (2020) 1–24 119728.
[15] W. Cao, C. Zhao, Y. Wang, T. Dong, F. Jiang, Thermal modeling of full-size-scale cylindrical battery pack cooled by channeled liquid flow, Int. J. Heat Mass Transfer 138 (2019) 1178–1187.
[16] A.A. Pesaran, Battery thermal models for hybrid vehicle simulations, J. Power Sources 110 (2002) 377–382.
[17] N. Javani, I. Dincer, G.F. Naterer, G.L. Rohrauer, Modeling of passive thermal management for electric vehicle battery packs with PCM between cells, Appl. Therm. Eng. 73 (2014) 307–316.
[18] T. Wang, K.J. Tseng, J. Zhao, Z. Wei, Thermal investigation of lithium-ion battery module with different cell arrangement structures and forced air-cooling strategies, Appl. Energy 134 (2014) 229–238.
[19] Z. Johnson, K. Ramakrishna, B. Joiner, M. Eyman, Thermal sub-modeling of the wirebonded plastic ball grid array package, in: Proc. 13th IEEE Semiconductor Thermal Measurement & Management Symp, 1997.
[20] H. Nishikawa, H. Serizawa, H. Murakawa, Actual application of FEM to analysis of large scale mechanical problems in welding, Sci. Tech. Welding Joining 12 (2007) 147–152.
[21] W. Schilders, H.A. Van der Vorst, J. Rommes, Model Order reduction: theory, Research Aspects and Applications, Springer, 2008.
[22] K. Zeng, D. Pal, H.J. Gong, N. Patil, B. Stucker, Comparison of 3DSIM thermal modelling of selective laser melting using new dynamic meshing method to ANSYS, Mater. Sci. Technol. 31 (2015) 945–956.
[23] S. Stoyanov, A. Dabek, C. Bailey, Thermo-mechanical sub-modelling of BGA components in PCB reflow, in: Proc. 36th. Int. Spring Seminar on Electron. Technol., 2013.
[24] M. Giglio, FEM submodelling fatigue analysis of a complex helicopter component, Int. J. Fatigue 21 (1999) 445–455.
[25] H. Wang, A. Li, R. Hu, J. Li, Accurate stress analysis on steel box girder of long span suspension bridges based on multi-scale submodeling method, Adv. Struc. Eng. 13 (2016) 727–740.
[26] Love, A., 'A Treatise On the Mathematical Theory of elasticity,', Cambridge University Press, 1927.
[27] S.J. Drake, M. Martin, D.A. Wetz, J.K. Ostanek, S.P. Miller, J.M. Heinzel, A. Jain, Heat generation rate measurement in a Li-ion cell at large C-rates through temperature and heat flux measurements, J. Power Sources 285 (2015) 266–273.
[28] V. Vishwakarma, et al., Heat transfer enhancement in a Lithium-ion cell through improved material-level thermal transport, J. Power Sources 300 (2015) 123–131.
[29] M. Parhizi, M.B. Ahmed, A. Jain, Determination of the core temperature of a Li-ion cell during thermal runaway, J. Power Sources 370 (2017) 27–35.
[30] S. Panchal, I. Dincer, M. Agelin-Chaab, R. Fraser, M. Fowler, Experimental temperature distributions in a prismatic lithium-ion battery at varying conditions, Int. Communic. Heat Mass Transfer 71 (2016) 35–43.
[31] D. Chalise, K. Shah, T. Halama, L. Komsiyska, A. Jain, An experimentally validated method for temperature prediction during cyclic operation of a Li-ion cell, Int. J. Heat Mass Transfer 112 (2017) 89–96.